

The Study of Target Shadows using Passive FSR Systems

Chr.Kabakchiev¹, I. Garvanov², V.Behar³, D. Kabakchieva⁴, K. Kabakchiev⁵,
H.Rohling⁶, K. Kulpa⁷, A. Yarovoy⁸

¹Sofia University, Sofia, BULGARIA
ckabakchiev@fmi.sofia-uni.bg

²University of Library Studies and Information Technologies Sofia, BULGARIA
i.garvanov@unibit.bg

³Institute of Information and Communication Technologies, Sofia, BULGARIA
behar@bas.bag

⁴University of World and National Economy, Sofia, BULGARIA
dkabakchieva@unwe.bg

⁵University of Birmingham, Birmingham, UK
kalin.kabakchiev@gmail.com

⁶Technical University of Hamburg-Harburg, Hamburg, GERMANY
rohlingr@tu-harburg.de

⁷Technical University, Warsaw, POLAND
kulpa@ise.pw.edu.pl

⁸Technical University, Delft, THE NETHERLAND
a.yarovoy@irctr.tudelft.nl

***Abstract:** The paper describes one possible algorithm for object detection by using of Forward Scatter (FS) radio shadows created by objects. The algorithm is verified on the experimental data collected by a GPS receiver with a small commercial antenna. The results obtained show the possibility for object detection when its FS shadow is present.*

1. Introduction

GPS-based Forward Scatter Radar (GPS FSR) is a specific case of passive bistatic radars, where GPS satellites are exploited as ‘transmitters of opportunity’. In GPS FSR systems, the bistatic angle between the directions "receiver-target" and "target-transmitter" should be around 180° , and such radar systems have very useful properties. Firstly, the receivers in GPS FSR are passive, and hence undetectable. Secondly, these radars can be potentially simple because GPS signals used for target detection cover the entire Earth surface. However, these radar systems have some limitations - lack of resolution in distance, the target must be very close to the baseline "transmitter-receiver". But these FS radars offer some features that make them interesting to study and use. Their most attractive feature is the sharp increase in the effective reflectivity of the object when it is near the baseline, leading to a dramatic amplification of the received signal from the object compared to traditional monostatic radar [1-9]. The idea to apply a GPS receiver to FSR for air target detection is discussed in [2]. Some experimental results of a GPS receiver concerning the detection of air targets are shown and discussed in [3]. A possible algorithm for air target detection in a GPS L5-based FSR system is described in [4], and the detection probability characteristics are calculated in [5] for the case when low-flying and poorly maneuverable (for example,

helicopters) air targets are detected on the background of a white Gaussian noise, or a Stand-off-Jammer (SOJ). Some experimental results concerning the study of radio shadows of some ground stationary and moving targets in civil environment are discussed in [6, 7, 8, 9].

Especially, this paper focuses on scientific issues related to new application of GPS in the construction and development of radar, which detects objects on their GPS radio shadows.

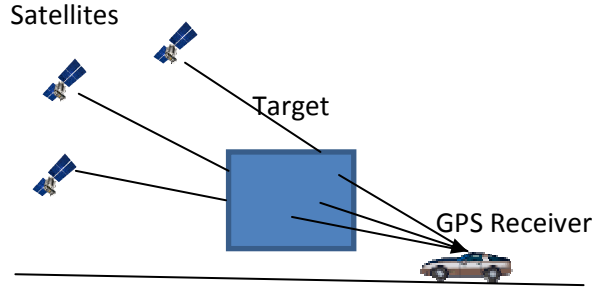


Figure 1: Topology of GPS FSR

The aim of the paper is to make experiments by a receiver of GPS-based FSR system (Fig.1) for recording GPS radio shadows created by objects and develop a possible algorithm for automatic detection of objects using their radio shadows. In such a system, the output signal of the Code&Carrier tracking block of a Software-Defined GPS receiver (GNSS SDR) after some transformation can be used for target detection using a target radio shadow. In this paper, a possible algorithm for automatic detection of radio shadows of ground targets, at the output of the Code&Carrier tracking block of a GNSS SDR, is described. The numerical results are obtained by processing the experimental data collected using the discrete component front end (GNSS SDR recorder) developed in the University of Colorado, Boulder, CO, USA and described in [10]. During the first experiment a car with GNSS SDR recorder travels at 60-70 km/h under a bridge with one band. During the second experiment the same car travels under a bridge with two separated bands. The radio shadow created by a bridge is used for bridge detection.

2. Signal Processing

The general block-scheme for target radio shadow detection using a Software-Defined GPS receiver is shown in Fig.1

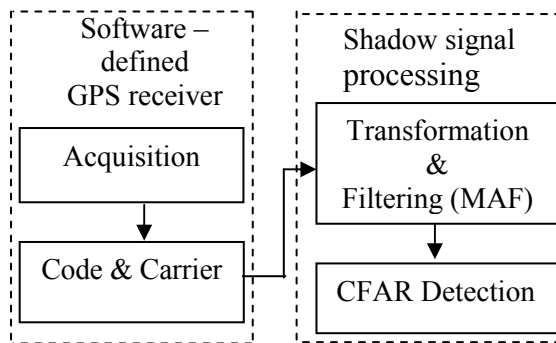


Figure 1: General block-scheme for target radio shadow detection

According to Fig.1, in the software-defined GPS receiver, the signal I_p at the output of the Code&Carrier block is obtained in result of execution of a set of program files for acquisition and tracking, presented in [10]. The signal I_p is further transformed as follows:

$$y = [(x - \max(x))]^2, \text{ where } x = \text{abs}(I_p) \quad (1)$$

This transformation is necessary for further signal detection by CFAR detector. As will be shown later, the Signal-to-Noise Ratio (SNR) is quite not enough for reliable signal detection. In order to improve SNR at the CFAR detector input, the signal y is filtered by the Moving Averaging Filter (MAF) [11]. The output signal of the MAF is described as:

$$y_{MAF}(n) = \sum_{k=-N}^N y(n-k)/(2N+1) \quad (2)$$

The filter impulse response in the time domain is $1/(2N+1)$, where $(2N+1)$ is the moving window length of the filter. The key problem is the optimal choice of the moving window length, i.e. N . When choosing the window length of the MAF we must take into account not only the level of suppression of the noise variance, but the degree of distortion of the useful signal immersed in noise. If f_{cut} is the highest frequency of the signal at the MAF output, then the improvement in SNR at the MAF output can be expressed as:

$$K(N) = \frac{1}{2N+1} \left(1 + 2 \sum_{k=1}^N \cos\left(\frac{2\pi k f_{cut}}{f_s}\right)\right)^2 \quad (3)$$

From (3) follows that the optimal window size, i.e. $(2N_{opt}+1)$ must be determined according to the following optimization criterion:

$$N_{opt} = \max \{K(N)\}_N \quad (4)$$

The CFAR detection approach is based on the criterion of Neyman – Pearson. According to this criterion, the following algorithm can be used for testing a simple hypothesis H_1 (target is present) against a simple alternative H_0 (target is absent):

$$\begin{aligned} H_1 : & \text{if } \max \{y_f(n)\} \geq T_{fa} \cdot \sum_{l=1}^L y_f'(l) \\ H_0 : & \text{otherwise} \end{aligned} \quad (5)$$

In the decision rule (5), $y_f'(l)$ are the values of the filtered signal within the reference window of size L needed for power noise estimation. The detection constant T_{fa} is determined in accordance with the probability of false alarm P_{fa} , which should be maintained by the detection algorithm. In case of mean zero Gaussian noise present in I_p , the detection constant can be calculated as:

$$T_{fa} = P_{fa}^{-1/L} - 1 \quad (6)$$

3. Experiment Description and Results

First experiment. During this experiment, a car with the GNSS SDR signal recording system travels at 60-70 km/h under a bridge with one band (Fig.2). Using the receiver AEK-4R, we can monitor the location of satellites (Fig. 3) and choice an appropriate satellite, the signal from which will be record by the GNSS SDR signal recording system.



Figure 2: Topology of the 1st experiment

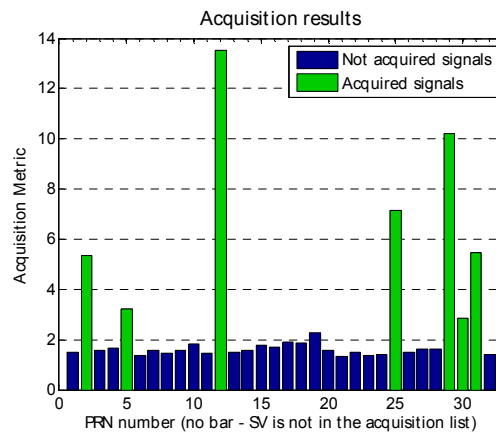


Figure 3: Satellite constellation

During this experiment the GPS SDR recording system records the signals received from three visible satellites (12, 29 and 25) as shown in Fig.3. The I_p components at the output of the Code&Carrier tracking block obtained for these satellites are shown in Fig.4. The satellite 29, whose elevation is in the range of 40^0 is used for the further signal processing.

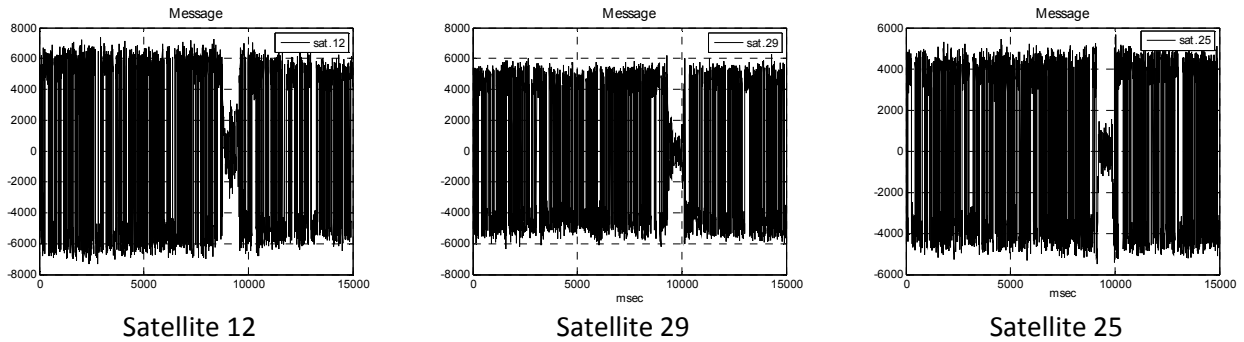


Figure 4: The I_p component at the Code&Carrier tracking block output of the software-defined GPS receiver

The I_p component of satellite 29 transformed according to (1) is shown in Fig.5 The corresponding spectrum of the transformed signal is shown in Fig.6.

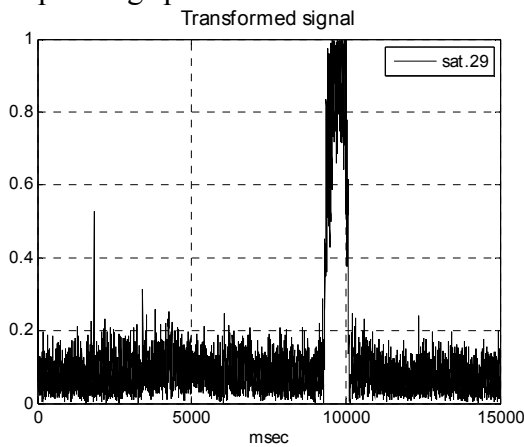


Figure 5: The transformed signal from satellite 29

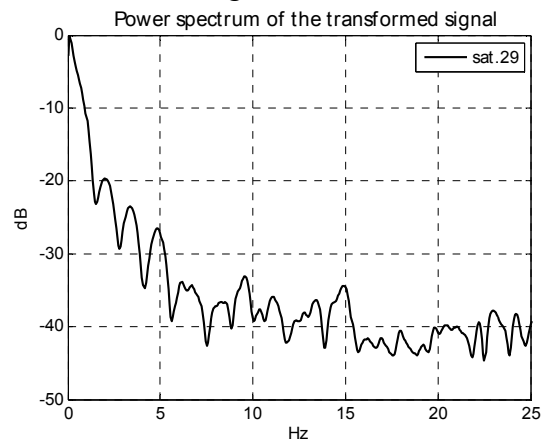


Figure 6: The spectrum of the transformed signal

The optimized values of N for determination of the MAF window length are calculated in accordance with the optimization criterion (4) and plotted in Fig.7 as a function of the cutoff frequency of the MAF. The corresponding values of the improvement factor in SNR at the filter output are plotted in Fig.8 as a function of the optimal parameter N .

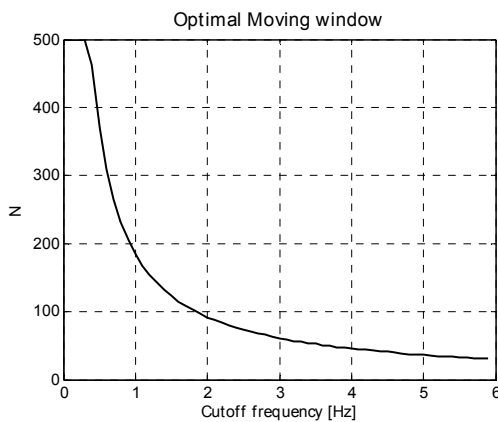


Figure 7: Optimal values of N as a function of f_{cut}

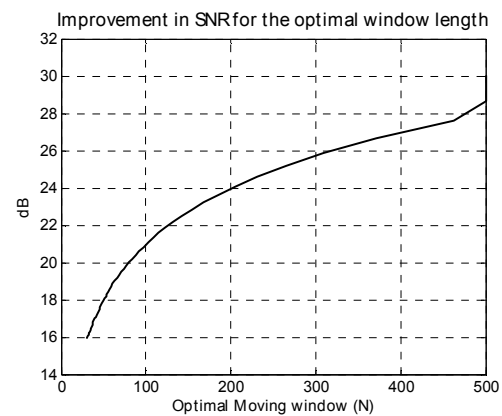


Figure 8: Improvement factor in SNR as a function of N

For comparison, two values of the filter cutoff frequencies are chosen from the spectrum shown in Fig.6 - 1.5 Hz and 5.6Hz. From Fig.7 follows that $N=123$ - for the cutoff frequency of 1.5 Hz, and $N=33$ - for the cutoff frequency of 5.6 Hz. The output signal of the moving

averaging filter together with the corresponding CFAR thresholds is shown in Fig.9 – for $N=123$ and in Fig.10 – for $N=33$. In the two cases the CFAR threshold is calculated for the false alarm probability of 0.001.

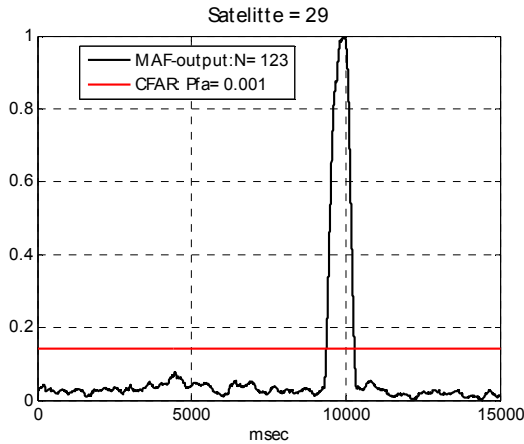


Figure 9: MAF output for $N=123$

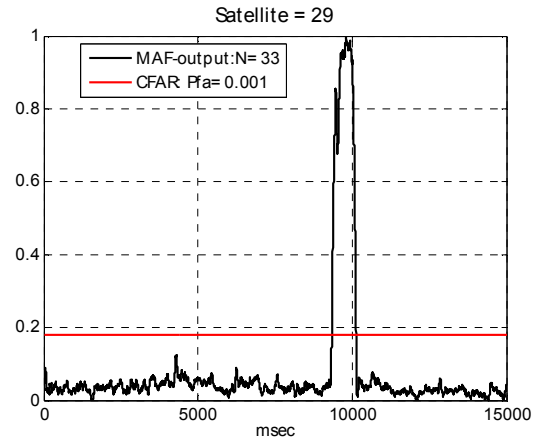


Figure 10: MAF output for $N=33$

The results shown in Fig.9 and Fig.10 show that the radio shadow created by a bridge can be used for its detection by the GNSS SDR.

Second experiment. During this experiment, a car with the GNSS SDR signal recording system travels at 60-70 km/h under a bridge with two separated bands (Fig.11). The satellite constellation during this experiment is shown in Fig.12.



Figure 11: Topology of the 2nd experiment

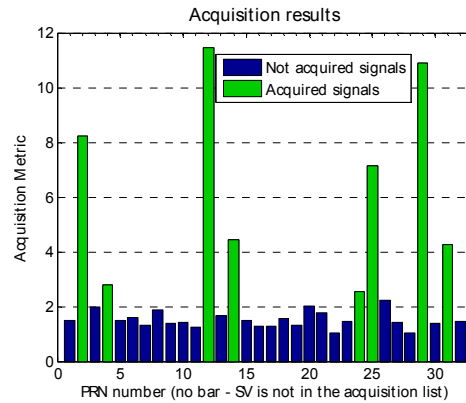


Figure 12: Satellite constellation

The values of the component I_p at the Code&Carrier tracking block of the software-defined GPS receiver are shown in Fig.13 for the three visible satellites – 12, 29 and 2.

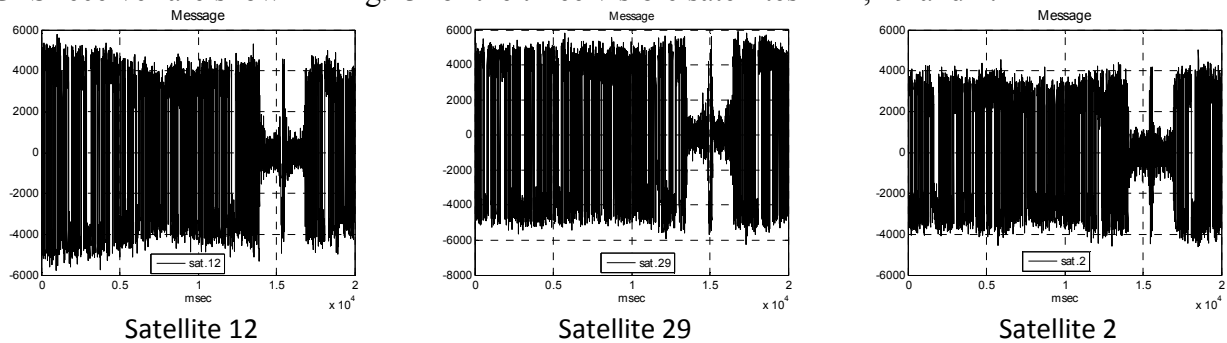


Figure 13: The I_p component at the Code&Carrier tracking block output of the software-defined GPS receiver

The signal from satellite 12 is chosen for signal processing. The signal at the MAF output together with the corresponding CFAR thresholds are plotted in Fig. 14 – for $N=123$ and in Fig. 15 – for $N=33$. The CFAR thresholds are calculated for $P_{fa}=0.001$.

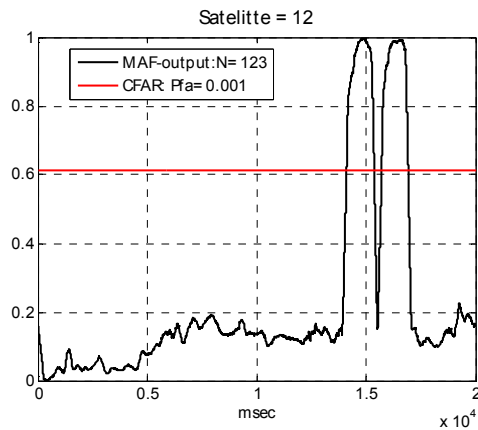


Figure 14. MAF output for $N=123$

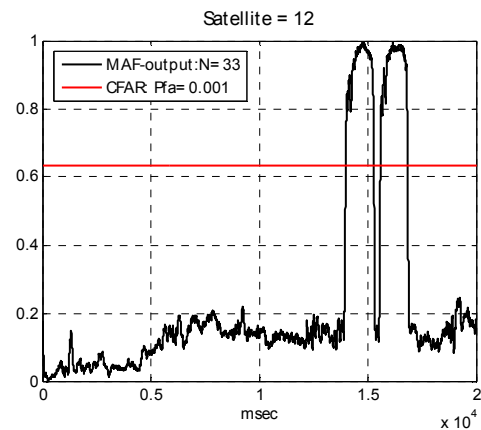


Figure 15: MAF output for $N=33$

It can be seen that two targets (two bands of the bridge) are usefully detected using the radio shadow created by the bridge. It can be seen that the topology of the two experiments satisfies the requirements for the occurrence of FS radio shadow, i.e. the objects are located close to the line „ satellite-GPS receiver”.

3. Conclusion

The paper shows that using a small commercial GPS antenna and the software-defined GPS receiver it is possible to detect different objects on their GPS radio shadows.

Acknowledgment

This work is partly supported by the project FNI T 02/2014.

References:

- [1] M. Cherniakov, (ed.), “Bistatic Radar: Principles and Practice”, Wiley & Sons, 2007.
- [2] V. Koch, R. Westphal, “New approach to a multistatic passive radar sensor for air/space defense”, *IEEE AES Systems Magazine*, November 1995, pp. 24-32,
- [3] I. Suberviola, I. Mayordome, J. Mendizabal, “Experimental results of air target detection with GPS forward scattering radar, *IEEE Geoscience and Remote Sensing Letters*, January 2012, vol. 9, no. 1, pp.47-51.
- [4] V. Behar, Chr. Kabakchiev, “Detectability of Air Target Detection using Bistatic Radar Based on GPS L5 Signals”, *Proc. IRS'2011*, Leipzig, 2011, pp. 212-217.
- [5] V. Behar, Chr. Kabakchiev, H. Rohling, “Air Target Detection Using Navigation Receivers Based on GPS L5 Signals”, *Proc. of ION GNSS' 2011*, Portland OR, 2011, pp. 333-337.
- [6] C. Kabakchiev, I. Garvanov, V. Behar, H. Rohling, “The Experimental Study of Possibility for Radar Target Detection in FSR Using L1-Based Non-Cooperative Transmitter”, *Proc. of IRS'13*, Dresden, Germany, 2013, pp.625-630.
- [7] C. Kabakchiev, I. Garvanov, V. Behar, H. Rohling, A. Lazarov, “The Experimental Study of Target FSR Shadows Detection using GPS signals”, *Proc. of the Third International Symposium on Radio Systems and Space Plasma*, Sofia, Bulgaria, 2013, pp. 64-73.
- [8] Ch. Kabakchiev, I. Garvanov, V. Behar, P. Daskalov, H. Rohling, “Moving Target FSR Shadow Detection using GPS signals”, *Proc. of Third International Conference on Telecommunications and Remote Sensing*, 26-27 June, 2014, Luxembourg, , pp. 34-40.
- [9] C. Kabakchiev, I. Garvanov, V. Behar, “Study of Moving Target Shadows using Passive Forward Scatter Radar Systems“, *Proc. IRS'2014*, June 16-18 , Poland, Gdansk, pp. 345-348.
- [10] K. Borre, D. Akos, N. Bertelsen, P. Rinder, S. Jensen, “A Software-Defined GPS and Galileo Receiver: Single-Frequency Approach”, Birkhäuser, Boston, MA, 2006.
- [11] <http://www.gaussianwaves.com/2010/11/moving-average-filter-ma-filter-2/>